Universitat Politècnica de Catalunya (UPC)
Universitat Autònoma de Barcelona (UAB)
Universitat de Barcelona (UB)
Institut de Ciències Fotòniques (ICFO)

http://www.photonicsbcn.eu

Master in Photonics

MASTER THESIS WORK

PLASMONICALLY ENHANCED ABSORPTION IN COLLOIDAL METAL/SEMICONDUCTOR NANOCOMPOSITES

F. Pelayo García de Arquer

Supervised by Dr. Gerasimos Konstantatos, (ICFO)

Presented on date 9th September 2010

Registered at

Escola Tècnica Superior d'Enginyeria de Telecomunicació de Barcelona

Plasmonically enhanced absorption in colloidal metal/semiconductor nanocomposites

F. Pelayo García de Arquer

ICFO - The Institute of Photonic Sciences, Mediterranean Technology Park Av. del Canal Olímpic s/n 08860 Castelldefels (Barcelona), Spain

E-mail: pelayo.garciadearquer@icfo.es

Abstract. Colloidal Quantum Dots (CQDs) are the route for low cost high efficiency photodetectors. Photoconductors are limited by the noise arising from high dark current densities, what is typically overcome reducing device's active area. However, this technique also reduces their photoresponse, and their optical absorption must be maintained as the volume is reduced. We study the use of plasmonics for that purpose, and present simulation results for solution-processed structures compatible with these techniques, showing up to a 13-fold enhancement in absorption. We present experimental results of a PbS CQDs photoconductor, fabricated using a novel CQDs functionalization, and venture the potential of these devices complemented with the shown promising techniques.

1. Introduction

Solution-processed nanostructured photonic materials have paved the way for low-cost high performance photodetectors [1, 2]. CQDs, solution-treated semiconductor nanoparticles (NPs) featuring quantum confinement of electrons/holes, have unique electrical and optical properties. There are many advantages of this technology compared to traditional semiconductors or epitaxially grown quantum dot materials. First, CQDs posses a very strong bandgap size-dependence, which allows spectral absorption tunability by adequately controlling NPs geometrical parameters and composition [3]. This feature is of key importance, as it ultimately serves to overcome infrared absorption limits of crystalline silicon devices. Second, self-assembly fabrication together with solution-cast processing make the production of such devices versatile, cost-effective and large-scalable, still being compatible with silicon electronics or with organic flexible substrates. Simple and low temperature chemistry plus device engineering led to momentous detectivities ($D^{\star}$, see table 1), even outperforming their best epitaxial counterparts [1]. All of these properties make CQDs an ideal candidate for efficient and economic photodetectors or photon sources. Yet to be fully exploited, CQDs photodetectors performance is asymptotically approaching its fundamental limits. Further improvements are bound either to breakthroughs in material science or to the combination of this technology with other disciplines, which could enhance and complement the huge potential of this field.

Table 1. Photodetector definitions and figures of merit.

Name	Expression	Units	Definition
Dark current (I_d)		A	Current without illumination
Responsivity ($\Re$)	$(I_l(\lambda) - I_d)/P_{inc}$	A/W	Photocurrent per incident optical power
EQE	$hc\Re/(\lambda q)$	-	Ratio of photocurrent to incoming photon rate
NEP	$I_{n,rms}/\Re/q$	$W/\sqrt{Hz}$	Noise Equivalent Power (minimum detectable power)
Normalized detectivity ($D^\star$)	$\sqrt{A_d B}/NEP$	jones (cm $Hz^{1/2}$/W)	Detector's sensitivity normalized to area A_d and bandwidth B

1.1. Current photodetectors limitations

Depending on the photodetector structure one can distinguish between photoconductors and photodiodes. Although their ultimate purpose is an efficient photon to carrier conversion, they have different working principles and characteristics. Table 1 introduces a list of figures of merit (FOM) and definitions for photodetectors. The most well understood and simpler photodetector is the the photoconductor, in which absorbed optical radiation causes a corresponding conductance or resistance change. Photoconductors are capable for high gain because long circulating carrier lifetimes. One type of charge carrier is able to circulate through an external circuit many times before it recombines. This fact serves to overcome the noise generated in read-out circuits, but also limits devices' bandwidth. The main constraint in photoconductors' performance comes however from their high dark current densities, proportional to A_d. Thus, it is of interest to reduce A_d, but reducing photoconductor's volume would also reduce the optical absorption, and thus the responsivity. Mechanisms to enhance the absorption for a given volume are therefore required to simultaneously achieve low noise but maintaining device's optical cross section, what implies an increase in the responsivity. In fact, not only photoconductive photodetectors can benefit of that. Enhanced absorbers attracted also the attention of the solar cell community, where the interest of volume reduction comes from the cost side, and it is considered to open a route to low cost efficient photovoltaics [4].

1.2. Plasmonics

Surface plasmons are excitations of the conduction electrons at the interface between a metal and a dielectric. If properly excited, these electron cloud oscillates coupled with an electromagnetic field highly confined to the metal-dielectric interface [5]. Surface plasmon polaritons (SPPs) propagate at this interface and are very sensitive to material properties, although they cannot be directly coupled to light. If the interface however is not planar, as it happens for metallic NPs, its geometry determines a restoring field because of the shifted oscillating electrons, leading to the so-called localized surface plasmon resonance (LSPR). This resonance, typically found the visible-IR, is also very sensitive to material's properties and environment, but it is mainly determined by the shape and size of the metallic particle.

Both SPPs and LSPR are in their nature sub-wavelength phenomena. That means that the induced λ_{SPP} or λ_{LSPR} of the sustained plasmonic modes are smaller than the free wavelength (λ_0), thus allowing light manipulation with diffraction-limited-less structures much smaller than λ_0. This feature has been touted to allow nano photo-electronic circuits integration [5]. Another aspect of great interest is the near field enhancement occurring within metal nano structures or NPs vicinity when on-resonance. This subwavelength localized and reinforced field opened a tremendous range of opportunities in applications such as biosensing or single-molecules study.

1.3. Plasmonically enhanced photodetectors

Given the properties of LSPR and SPPs, Plasmonics offers the possibility to overcome current photodetector limitations [2, 4]. First, metallic NPs can be used as subwavelength scattering elements to couple and trap impinging photons to the semiconductor, increasing its effective absorption cross section (see Fig. 1a). If adequately designed NPs are placed close or at the interface of two dielectrics, scattering preferably occurs into the dielectric with the larger permittivity. Moreover, the scattered light acquires an angular spread, effectively increasing the optical length or even trapping light beyond the critical angle limit. For this mechanism to be effective, NPs size has to be big enough so the scattering cross section (which scales with the square of NPs volume, V_{NP}^2) is bigger than the absorption inside the NPs (proportional to V_{NP}). The fraction of light scattered into the substrate is very sensitive to the shape and size of the NPs, found best for hemispherical and cylindrical particles [4]. Instead of metal NPs, other structures can also be used to take advantage of the plasmonic enhanced evanescent fields. Hole or ridge patterned metal layers above a semiconductor absorbing film have been also reported to successfully enhance light conversion efficiency [6].

Alternatively, the use of strong local field enhancement and near field coupling around metal NPs can increase absorption in a surrounding semiconductor material (Fig. 1b). This is optimized for small particles (typically less than 20 nm diameter), which better transfer the incoming energy to a localized surface plasmon mode [4]. The interaction between these NPs can also be exploited to tune the absorption spectrum.

Third, light can be converted into propagating SPPs at the photodetector metallic back-contact/semiconductor interface (Fig. 1c). To achieve this, the SPPs-free light momentum mismatch has to be attained by introducing subwavelength gratings or other corrugations in the metal contact [7]. Near resonance, SPPs evanescent electromagnetic fields are confined at this interface turning the incident power flux by 90º.

Finally, metallic structures can be designed to focus incoming light into subwavelength volumes thanks to plasmonic effects, much like an antenna (Fig. 1d). The enhanced and focused near field allows for ultra-small photodetectors, with low noise and dark current, high speed, but on the other hand the same absorbing cross section [8].

2. State of the art

Investigation in the area of CQDs photodetectors is mainly focused either in the improvement of current materials' properties, or in the search of new ones, able to produce cheaper, more

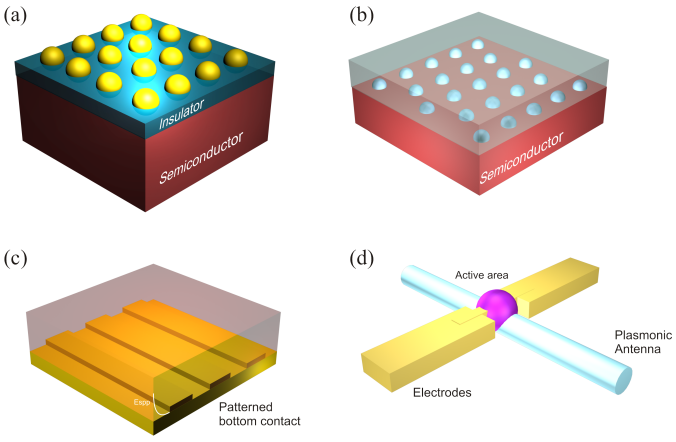

Figure 1. Approaches to enhance photodetection by the use of plasmonics. (a) Scattering from metal NPs can be employed to increase the amount of light coupled to the semiconductor, also increasing photon's optical length. (b) Near-field enhancement associated to the LSPRs can increase semiconductor absorption for some wavelenghts. (c) Corrugations in the metal contact can convert light to SPPs propagating at metal/semiconductor interface, increasing semiconductor absorption due to SPPs evanescent fields in the vertical direction. (d) Plasmonic "lenses" can be used to focus light into subwavelength apertures, allowing ultra small volume absorbing detectors.

effective, and more stable devices [2]. The so far commented plasmonics potential improvements have been however mainly experimentally studied for the family of Si photodetectors, specially for solar cells [4, 9–11]. Following the first exposed scheme in the previous section, Stuart *et al* reported in [9] a 12-fold enhancement in solar cell short-circuit current (J_{SC}). They utilized metal islands over a 0.16 μm thick Si layer of a silicon-on-insulator wafer, and determined the best case to happen for Cu at 800 nm. In [10] a 97% increase in the photocurrent of a silicon nanocrystal photodetector is attributed to the introduction of metal Ag islands formed on Si-wafers, found optimum for 90 nm size. In [11] Ferry *et al* modify a solar cell back scatterer by Ag patterning on the rear glass substrate. A 50% increase in J_{SC} is achieved for a 500 nm defect pitch compared to that of an unpatterned device. Also the performance of organic solar cells [12] or epitaxial quantum dot devices [6] have been shown to increase elsewhere by using either one of these methods. In [6], Chang *et al* report a 130% enhancement in the infrared photoresponse of an InAs QD photodetector, arising from the introduction of a gold hole-array drilled layer on top of the device.

Following the plasmonic antenna-concentrator approach (Fig. 1d), enhanced photocurrent is shown in [8] among others. Tang *et al* manage to get a 20 fold increase in the photocurrent of a subwavelength ultra small (of the order of $1 \times 10^{-4}\lambda^3$) germanium photodetector by using a Hertz dipole antenna ($L_{dip} \simeq 380\ nm$). This small volume allowed for high-speed operating device (bandwidth $\simeq$ 150 GHz). Theoretical and simulation results also predicted absorption enhancements up to 1000% with similar subwavelength-focusing techniques [13].

Although general, these improvements rely mainly on the introduction of metal NPs, either on top of device or into an absorbing semiconductor layer. It is critical that any of

these modifications do not alter CQDs intrinsic advantages, such as low-cost, scalability and integrability [2]. In that trend, few attempts have been made yet to join plasmonic potential improvements with CQDs.

In 2008 Lee *et al* [14] studied the properties of core-shell PbS-Au photodetector. They compared optical and electrical properties of this strongly confined metal-semiconductor structure with that of its individual building blocks. A 28% absorption enhancement was found, together with an Au plasmon peak for the PbS-Au system. However, this increase is global and due to the fact that gold has a bigger absorption than PbS, and no photocurrent enhancement was proved. The major result of their work is the controlled p-doping of PbS by the introduction of the gold core particles.

In the subsequent sections, first, we will study the possibilities of plasmonic enhancement for two families of devices with full-wave electromagnetic simulations. The properties of CQDs PbS/Au-Cu nanocomposites will be analyzed for absorption increase, yielding up to a 4-fold enhancement. Another promising material, Cu-Cu_2O core-shell system will be characterized. This NPs are of high interest, as its intrinsic semiconductor-metal structure allows for natural plasmonic enhancement due to Cu oxidized layers as the surrounding of a metal core. A 13-fold enhancement is predicted for that material.

We conclude our study with an experimental demonstration of a PbS photodetector based on a novel NPs functionalization, to serve as a baseline case to integrate the plasmonic proven enhancement techniques in a future work.

3. PbS + Metal photoconductor

CQDs PbS are of huge interest because lead-salts abundance on earth and proved outstanding performance [1]. PbS offer photoconductive gain and high size-tunable spectrum (from Vis to IR). The absorption in a solution-processed layer of PbS will be simulated, and the plasmonic effects of an embedded set of metallic NPs analyzed with FDTD simulations (Lumerical Solutions 6.5).

PbS quantum dots were modeled with its particle-size dependant refractive index, characterized by using the Kramers-Kronig relation from an in-solution absorbance measurement (see section 7). This batch showed its exciton peak at $\lambda = 1069$ nm. The obtained complex refractive index values were later fitted by the program with a multi-coefficient polynomial. NPs refractive index data is taken from CRC (Cu) and Johnson&Christy (Au). A 90 nm thick layer of PbS nano crystals with 3 nm diameter, estimated as a first approach of NPs size, were organized following face centered cubic (FCC) or hexagonal packing schemes. The PbS film is embedded in vacuum and illuminated with a plane wave (Fig. 2(a)). An unit cell of side W and thickness 1200 nm is taken and boundary periodic boundary conditions applied in $x-y$ directions. Boundaries in the z direction are set to perfectly matched layer. A fine mesh of 0.25 nm brick side is applied to a $16 \times 16 \times 90\ nm^3$ box containing 4 metallic NPs (none for the base case) of 9 nm size distributed uniformly inside the layer. A coarser automatic mesh is applied for the rest of the unit cell. The ratio of absorbed power in the semiconductor to input power, ($\eta_{abs} = P_{abs}/P_{inc} = \frac{\omega}{2P_{inc}(\lambda)} \int_{V_{SC}} \epsilon''(\lambda)|E(\mathbf{r},\lambda)|^2 dV$), where $|E|^2$ is the intensity of the electric field, ϵ'' the imaginary part of permittivity, P_{in} the incident

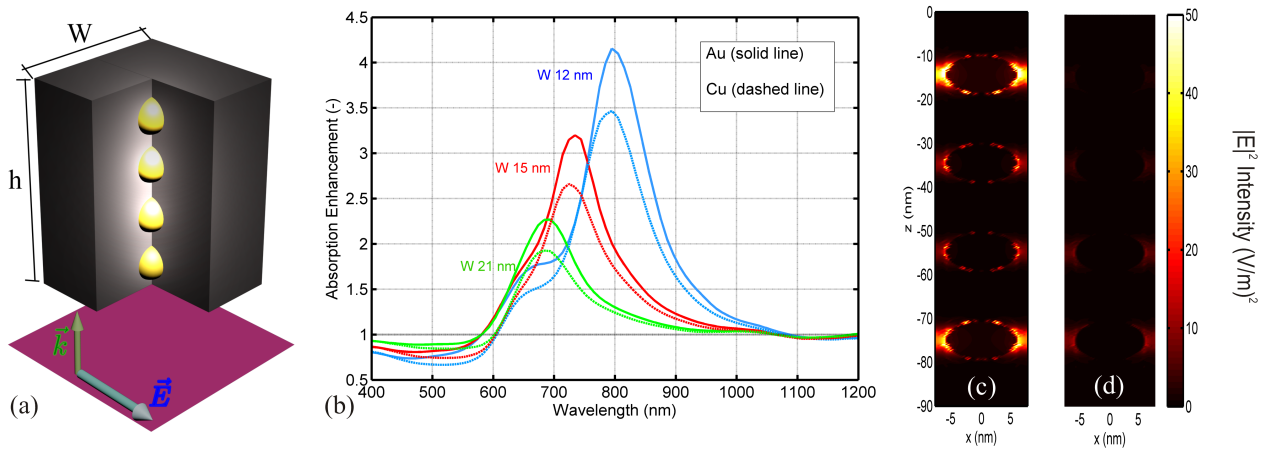

Figure 2. Plasmonic absorption enhancement for PbS-metal NPs nanocomposite. (a) Schematic of the unit cell simulation setup. A PbS nanocrystals (3 nm diameter) layer with hexagonal packing, width $W_x = W_y = W$ and thickness $h = 90$ nm is embedded in vacuum and illuminated with a plane wave ($\vec{E} = E\hat{x}$, $\vec{k} = -k\hat{z}$). Periodic boundary conditions are applied in x and y directions. Four metallic spheres of 9 nm size are distributed uniformly in the z direction (see section cut). By varying W the effects of metallic NPs concentration in the absorption are studied. (b) Ratio of absorbed power in PbS with metal NPs (Au-solid line, Cu-dashed line) to bare PbS absorption. Au yields higher and slightly redshifted enhancements than Cu. The closer are the NPs the bigger the plasmonic contribution. Near field intensity enhancements for $W = 12$ nm and Cu NPs are shown in (c) and (d) for $\lambda = 800$ nm and $\lambda = 1100$ nm respectively. Peak intensity is 160 $(V/m)^2$ but colorbar has been limited to allow a better comparison.

power and V_{SC} the semiconductor volume, will be used as a figure of merit. This expression is only valid for non-magnetic materials, which is the case. Figure 2b plots the PbS absorption enhancement after metal NPs introduction ($\eta_{abs,NP}/\eta_{abs,0}$) for hexagonal packing (best case). Gold shows a higher increase than Cu, about 14%, attributed to its slightly smaller absorption coefficient in the wavelengths of interest. As W is reduced (NPs closer to each other in the $x-y$ plane, thus more concentrated), NPs near field interaction enhance PbS absorption in the wavelengths corresponding to the LSPR of these metals embedded in a PbS host ($n_{PbS} \simeq 2.5$). 4 fold increase in absorption can be achieved when $W = 12$ nm for Au NPs. In other spectral regions (aprox. $\lambda < 600$ nm) the effect of the metal NPs is negative, as Au and Cu show greater absorption. For longer wavelengths ($\lambda > 1100$ nm), as the PbS absorption approaches zero and NPs conductivity increases, no enhancement is evident. Metal NPs interaction and near field intensity is shown in Fig. 2(c-d) for $\lambda = 800$ and $\lambda = 1100$ nm respectively. Peak intensities of 160 $(V/m)^2$ appear for the first case, whereas for the latter 10 $(V/m)^2$ is the maximum.

4. Cu/Cu2O core-shell photodetector

Copper is one of the most abundant materials in Earth's crust. Cuprous oxide (Cu_2O) is a p-type semiconductor that naturally appears from copper oxidization. The synthesis of colloidal Cu_2O NPs is then of great interest, as it will merge solution-processing advantages with cheap materials [15]. However, Cu_2O absorption strongly decays above $\lambda = 600$ nm, coinciding with

the region where Cu LSPR can arise. If properly controlled, oxidization of Cu NPs can lead in an easy manner to core-shell metal-semiconductor Cu-Cu_2O systems (Fig. 3-a), with highly tunable LSPR, that could serve to overcome Cu absorption bandgap limitation by plasmon-carrier energy transfer (Fig. 3-b).

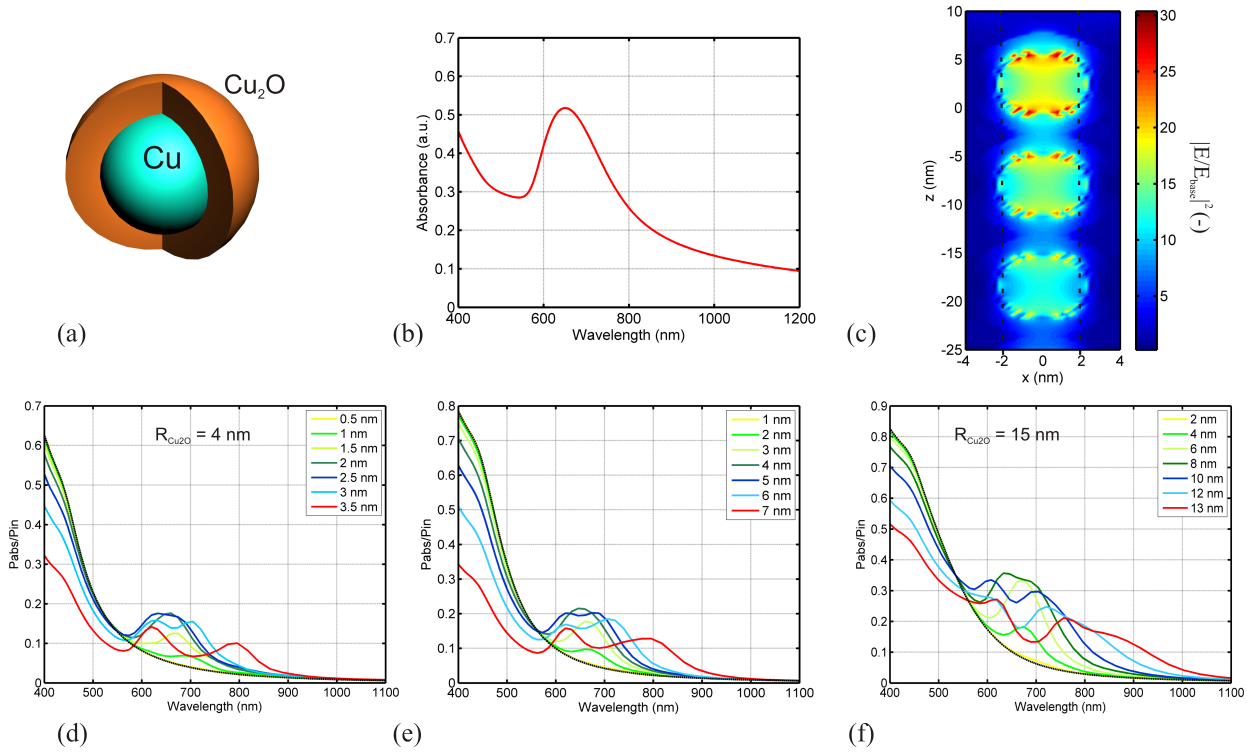

Figure 3. Cu-Cu_2O core-shell structure optical properties. (a) Synthesized Cu NPs self oxidize resulting in a Cu_2O shell of variable thickness. (b) Absorbance of drop-casted Cu-Cu_2O oleic acid capped NPs on glass substrate. Oleic acid protects from self-oxidation, and a clear plasmonic peak is observed around 640 nm at normal conditions. (d) Field enhancement of the system with a Cu core (R_{Cu} = 2 nm, R_{Cu_2O} = 4 nm) respect the fully oxidized at λ = 660 nm. In the Cu_2O shell local 14 fold enhancement is achieved. Incident electric field x-polarized. Absorbed to incident power ratio spectra is shown in (e-g) for different sizes and aspect ratios, together with no Cu (black-dashed line) for comparison. (e) $R_{Cu_2O} = 4\ nm$, (f) R_{Cu_2O} = 8 nm, (g) R_{Cu_2O} = 15 nm. Up to an 8-fold enhancement at 900 nm is achieved when R_{Cu} = 13 nm, R_{Cu_2O} = 15 nm

A 90 nm thick layer of Cu-Cu_2O NPs with sizes of 8 nm, 16, nm and 30 nm is simulated with periodic boundary conditions (as done in section 3) for different core-shell NPs aspect ratios. Fig. 3-c shows the field intensity enhancement for $R_{Cu_2O} = 4\ nm$ and $R_{Cu} = 2\ nm$, compared to the fully oxidized system at Cu LSPR ($\lambda \simeq 660$ nm). Up to 10-fold relative increase areas are present in z direction in Cu_2O volumes. Figs3-d-f plot Cu_2O absorption for different NPs sizes and aspect ratios $\Delta = R_{Cu}/R_{Cu_2O}$. Two regimes are observed. For $\Delta < 0.5$ enhancement peak is due to the fundamental LSPR mode on Cu-Cu_2O, and blueshifts and increases with Δ. When $\Delta > 0.5$ hybridized plasmonic modes gain presence and the peak is split in two, with lower and higher energies. Higher relative enhancements occur for higher Δ for the red-shifted modes, but as a counterpart absorption in Vis-UV decreases. Up to an 8-fold enhancement

at 900 nm can be achieved for $R_{Cu} = 13$ nm and $R_{Cu_2O} = 15$ nm. Thus, big particles with relatively high aspect ratios offer the possibility of higher and red-shifted enhancements in the IR. Cu-Cu_2O core-shell composites allow enhanced absorption engineering in the 600-1000 nm window, opening a potential way for low-cost tuneable solution-processed photodetectors.

5. Experimental results

A PbS CQD photoconductive photodetector was fabricated and electro-optically characterized. CQDs were spin-coated onto gold interdigitated electrodes (see Fig.4-a). PbS NPs were oleic-acid capped diluted in toluene (40 mg/mL) and pre-filtered prior to fabrication. Post-synthetic ligand exchange (LE) is performed by drop-casting ethanedithiol $C_2H_4(SH)_2$ (EDT) 1% volume diluted in acetonitrile (ACN) onto the sample. Remaining EDT is cleaned with ACN and not ligand-exchanged nanocrystals removed with toluene. Absorbance of an on-glass sample is shown in Fig.4-b inset, zoomed to its exciton peak ($\lambda \simeq 970$ nm). Two layers are built with this process. The thickness of the PbS film is between 20-30 nm. Our novel EDT LE approach has not been previously reported for CQDs photoconductors, and provides high sensitivity and gain devices in one-step fabrication solution process.

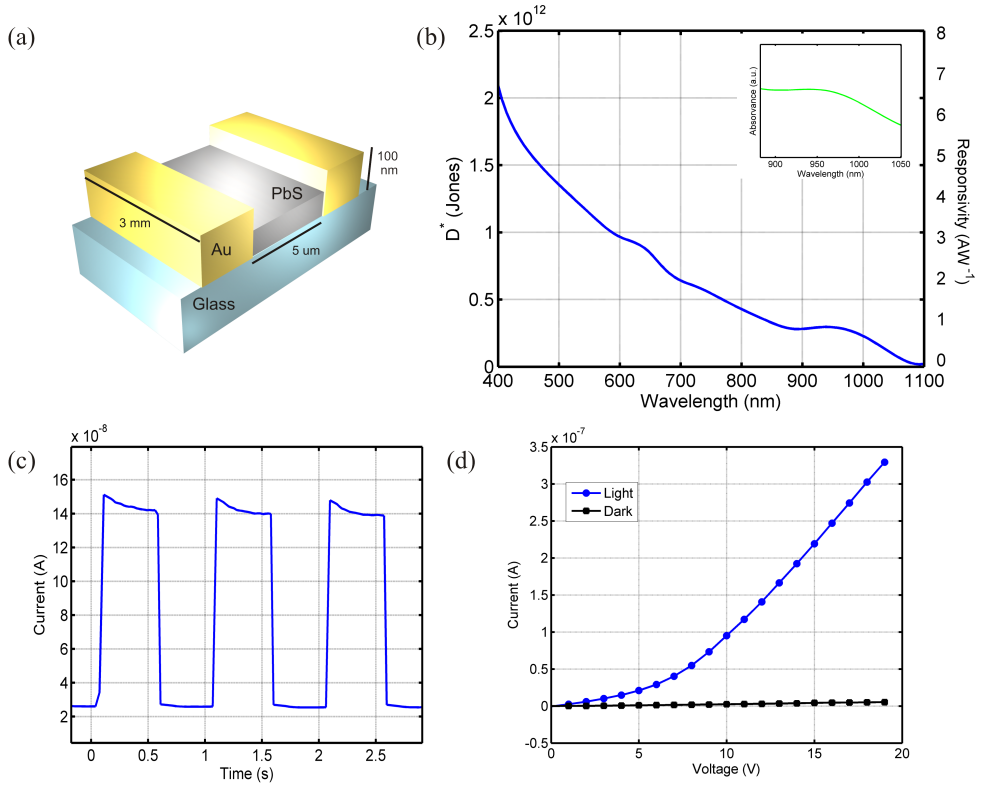

Figure 4. Device structure and its electro-optic characteristics. (a) Gold interdigitated electrodes (IDEs) are spin coated with PbS NPs. (b) $D^\star$ as a function of wavelength for 20 V bias. Inset shows exciton peak absorbance of a PbS on glass sample following steps described previously. (c) Current-time for 1 Hz modulation with 635 nm LASER illumination (d) Current-Voltage characteristic of fabricated device with 904 nm LASER illumination.

The device was 20 V biased and measured (see section 7). Photocurrent spectrum was

taken by illuminating the sample from 400 nm to 1100 nm in steps of 50 nm. The current (I) at 20 V is recorded as a function of time at each step, manually controlling monochromator's shutter to analyze dark-light-dark response. Dark current average value is of the order of 5 nA. Steady state values were taken for calculations. Device's responsivity is plotted in Fig.4-b (right-axis), and limited because of PbS thickness. First and second exciton peaks are clear at 970 nm and 620 nm respectively. Normalized detectivity is shown in the left axis, and is of the order of 10^{12} Jones. EQE is 125% at the first exciton peak, and 611% at second, accounting for photoconductive gain. Time response of the device is depicted in Fig.4-c at 20 V bias for 1 Hz modulated 904 nm LASER. Photocurrent clearly responds to light modulation, and complete relaxation occurs in less than 100 ms. Finally, the I-V characteristic of the device is plotted in Fig.4-d for 904 nm LASER illumination and dark conditions. The I-V shape is not linear but superlinear, which is characteristic of field-assisted transport, due to the presence of energetic barriers formed along the pathway of carrier transport [1].

Plasmonic improvements can be handily integrated with this family of photodetectors without loosing the benefits of CQDs. Metal NPs of a definite size can be added either in the solution phase (metal/semiconductor nanocomposites) or in layer by layer fabrication process. Cu, Au and Ag NPs are good candidates featuring LSPR resonances in different regions of the spectrum. However, the compatibility of these metal NPs with the functionalized CQDs host medium deserves a careful study beyond the timeframe of the present master thesis.

6. Conclusions and future work

Solution processed CQDs offer low-cost, high sensitive and tunable photodetectors. Main limitations in photoconductors come from their high dark current densities compared to other devices such as diodes. Reducing detector's volume lowers the noise, but decreases optical cross section and photoresponse. Plasmonics can over overcome this problem with the aid of metal NPs or other nanostructures. We studied potential improvements for the case of CQDs photodetectors, particularized for PbS-Au/Cu nanocomposites. Changing metal NPs concentration can tune the enhancement, up to 4-fold increase, typically found in the VIS-IR. Another type of structure consisting of Cu-Cu_2O core-shell nano crystals, were studied. A high degree of tunability of the enhanced absorption spectrum of this low-cost solution processed material was revealed, yielding 13-fold enhancements. A PbS CQD photoconductor was fabricated using novel LE compounds, and electro-optically characterized. This family of high sensitive ultra-thin devices can serve as a base to apply all the promising aforementioned improvements.

7. Methods

K-K relation was implemented by numerically calculating Cauchy's principal value using adaptative domain integration. Electrical measurements were performed with a Keathly 2626A source meter pico-amperimeter. A Cary 5000 Varian spectrometer was used for absorbance characterization. A Newport Oriel Apex monochromator was employed as source for responsivity measurements, LASER source for I-V characterization. All reagents were purchased from Sigma Aldrich and all the reactions were carried out using standard Schlenk techniques.

The synthesis of the Cu_2O NCs was performed following the previously reported procedure [15]. Syntheis of PbS NCs were carried out following the procedure previously reported [16].

8. Acknowledgements

I would like to thank Prof. Dr. Konstantatos for his supervision, guidance, and exciting discussions along this project. Also Luis Martínez, Dr. María Bernechea, and Dr. Xiaojie Yang, who have been always willing to help. All of this work would not have been possible without the support of "Fundación La Caixa" and their fellowship programs.

References

[1] G. Konstantatos, I. Howard, A. Fischer, S. Hoogland, J. Clifford, E. Klem, L. Levina, and E. H. Sargent, "Ultrasensitive solution-cast quantum dot photodetectors," *Nature (London)*, vol. 442, pp. 180–183, 2010.

[2] G. Konstantatos and E. H. Sargent, "Nanostructured materials for photon detection," *Nature Nano.*, vol. 5, no. 6, pp. 391–400, 2010.

[3] D. V. Talapin, J.-S. Lee, M. V. Kovalenko, and E. V. Shevchenko, "Prospects of colloidal nanocrystals for electronic and optoelectronic applications," *Chem. Rev.*, vol. 110, no. 5, pp. 686–688, 2010.

[4] H. Atwater and A. Polman, "Plasmonics for improved photovoltaic devices," *Nature Mat.*, vol. 9, no. 3, pp. 205–213, 2010.

[5] D. Gramotnev and S. Bozhevolnyi, "Plasmonics beyond the diffraction limit," *Nature Photon.*, vol. 4, no. 2, pp. 83–91, 2010.

[6] C.-C. Chang, Y. D. Sharma, Y.-S. Kim, J. A. Bur, R. V. Shenoi, S. Krishna, D. Huang, and S.-Y. Lin, "A surface plasmon enhanced infrared photodetector based on inas quantum dots," *Nano Lett.*, vol. 10, no. 5, pp. 1704–1709, 2010.

[7] H. Raether, *Surface plasmons on smooth and rough surfaces and on grattings*. 1988.

[8] L. Tang, S. E. Kocabas, S. Latif, A. K. Okyay, D.-S. Ly-Gagnon, K. C. Saraswat, and D. A. B. Miller, "Nanometre-scale germanium photodetector enhanced by a near-infrared dipole antenna," *Nature Photon.*, vol. 2, no. 4, pp. 226–229, 2008.

[9] H. Stuart and D. Hall, "Absorption enhancement in silicon-on-insulator waveguides using metal island films," *Appl. Phys. Lett.*, vol. 69, p. 2327, 1996.

[10] S.-K. Kim, C.-H. Cho, B.-H. Kim, Y.-S. Choi, S.-J. Park, K. Lee, and S. Im, "The effect of localized surface plasmon on the photocurrent of silicon nanocrystal photodetectors," *Appl. Phys. Lett.*, vol. 94, no. 18, p. 183108, 2009.

[11] V. E. Ferry, M. A. Verschuuren, H. B. T. Li, E. Verhagen, R. J. Walters, R. E. I. Schropp, H. A. Atwater, and A. Polman, "Light trapping in ultrathin plasmonic solar cells," *Opt. Express*, vol. 18, no. S2, pp. A237–A245, 2010.

[12] B. P. Rand, P. Peumans, and S. R. Forrest, "Long-range absorption enhancement in organic tandem thin-film solar cells containing silver nanoclusters," *J. Appl. Phys.*, vol. 96, no. 12, pp. 7519–7526, 2004.

[13] J. S. White, G. Veronis, Z. Yu, E. S. Barnard, A. Chandran, S. Fan, and M. L. Brongersma, "Extraordinary optical absorption through subwavelength slits," *Opt. Lett.*, vol. 34, no. 5, pp. 686–688, 2009.

[14] J.-S. Lee, E. V. Shevchenko, and D. V. Talapin, "Au-pbs core-shell nanocrystals: Plasmonic absorption enhancement and electrical doping via intra-particle charge transfer," *J. Am. Chem. Soc.*, vol. 130, no. 30, pp. 9673–9675, 2008. PMID: 18597463.

[15] L.-I. Hung, C.-K. Tsung, W. Huang, and P. Yang, "Room-temperature formation of hollow Cu2O nanoparticles," *Advanced Materials*, vol. 22, no. 17, pp. 1910–1914, 2010.

[16] J. Tang, L. Brzozowski, D. A. R. Barkhouse, X. Wang, R. Debnath, R. Wolowiec, E. Palmiano, L. Levina, A. G. Pattantyus-Abraham, D. Jamakosmanovic, and E. H. Sargent, "Quantum dot photovoltaics in the extreme quantum confinement regime: The surface-chemical origins of exceptional air- and light-stability," *ACS Nano*, vol. 4, no. 2, pp. 869–878, 2010.